

https://dspace.org/

Twomode averaging for turbulence resilience

Alice Drozdov; Mitchell Cox

OPTICAL SOC AMER
https://hdl.handle.net/10539/45521
WOS

Downloaded from a DSpace repository. https://dspace.org/

applied optics

Two-mode averaging for turbulence resilience

ALICE V. DROZDOV AND MITCHELL A. COX*

School of Electrical and Information Engineering, University of the Witwatersrand, Johannesburg 2050, South Africa
**mitchell.cox@wits.ac.za*

Received 29 May 2024; revised 7 October 2024; accepted 29 October 2024; posted 30 October 2024; published 15 November 2024

Atmospheric turbulence typically impairs free-space optical communication systems, particularly those using mode-division multiplexing, by causing detrimental crosstalk among higher-order modes. This interaction can also be harnessed through mode averaging at the receiver and transmitter to passively counteract turbulence effects. Mode averaging involves the simultaneous transmission and detection of multiple, strategically selected modes. Prior research on mode averaging—often referred to as modal diversity—primarily selected modes by using the spread of crosstalk among modes. In this study, we show that it is crucial to include the impact of mode-dependent loss. This is demonstrated by identifying optimal two-mode combinations that maximize received power while efficiently utilizing mode space. The optimal combinations assessed include pairs of orbital angular momentum (OAM), Laguerre-Gaussian (LG), and Hermite-Gaussian (HG) modes, as well as mixed pairs of LG and HG modes. Interestingly, it is shown that the optimal combinations are not always the neighboring modes. © 2024 Optica Publishing Group. All rights, including for text and data mining (TDM), Artificial Intelligence (AI) training, and similar technologies, are reserved.

https://doi.org/10.1364/AO.530685

1. INTRODUCTION

The use of higher-order modes such as orbital angular momentum (OAM), Laguerre-Gaussian (LG), and Hermite-Gaussian (HG) in free space optical communication has garnered significant interest [1]. A prominent area of study within this domain focuses on the transmission of superimposed modes, with each mode conveying distinct signals. This technique, known as mode-division multiplexing (MDM), aims to enhance the signal capacity [2]. However, its effectiveness is limited to short distances with minimal atmospheric turbulence, as higher-order spatial modes are prone to interference from turbulence, leading to crosstalk and errors [3].

Crosstalk involves the unwanted spread of energy from a transmitted mode to *adjacent* modes, diminishing the energy and intensity of the original signal. This phenomenon, coupled with mode-dependent loss (MDL) or fading, reduces the average received power of the signal and can lead to detection failures in free space optical (FSO) systems, manifesting as fading errors [4].

Efforts to mitigate these fading errors have led to the exploration of various strategies. These include adaptive optics [5], multiple input multiple output (MIMO) digital signal processing (DSP) [6], aperture averaging [7], and spatial diversity [8]. The complexity and cost of the required hardware limit the use of these mitigation techniques in practical FSO systems. Another technique is modal diversity, which capitalizes on the statistical independence of different modes [9]. Its use in FSO systems is limited as the technique is not yet fully understood.

A method similar to both modal diversity and aperture averaging involves transmitting and/or receiving several adjacent modes to mitigate the fading errors caused by MDL [10]. This method allows for the recovery of the power that has been coupled into adjacent modes [11], effectively collecting more light in a similar way to how aperture averaging does [12].

Although sometimes referred to as *mode diversity*, we prefer to call this technique *mode averaging*, as we are not leveraging the statistical independence of different modes in turbulence for diversity gain. It is more similar to aperture averaging than it is to modal diversity [7,12].

Mode averaging can be applied in various configurations: at the receiver by transmitting a single mode and detecting multiple modes [13,14], at the transmitter by transmitting several modes encoded with similar data and detecting only one [10], or simultaneously at both ends. Mode averaging at the receiver and transmitter involves transmitting multiple modes at the transmitter and receiving those modes at the receiver. As these modes pass through turbulence, power is lost from the transmitted modes via crosstalk into other modes. However, in a mode averaging system, some of the lost power remains in the system as it is coupled between the transmitted modes and received with them. The total received power, thus, comprises the power retained in the transmitted modes and the power coupled into them through crosstalk. The benefit of using mode averaging compared to many of the mentioned turbulence compensation techniques is that it passively compensates for turbulence.

Mode averaging at both the receiver and transmitter has been shown to decrease the average bit error rate (BER) when two or

three OAM modes are transmitted and received simultaneously compared to a system that only transmits a single mode [15]. Other studies have combined mode averaging with spatial diversity and/or MIMO [16–18], demonstrating an enhanced link robustness through a decrease in the outage probability. Two other studies combined mode averaging with MDM, showing that using mode averaging in addition to MDM helps decrease the BER and outage probability of a system using MDM [19,20]. Since mode averaging is likely to be utilized alongside MDM, in this work we limit ourselves to pairs of modes, leaving other (pairs of) modes for MDM [15,17,18].

While previous studies have demonstrated that incorporating more modes generally leads to better performance, utilizing just two modes for mode averaging at both the receiver and transmitter still yields significant improvements compared to a system without mode averaging, when comparing outage percentages [15,16]. The performance gain from using two modes is substantially larger than the additional gain achieved when increasing from two to three modes in a mode averaging system.

Many of the studies discussed are proof of concepts showcasing the use of mode averaging/diversity to improve the performance of communication systems in turbulence. In this work, we aim to advance these findings by optimizing mode averaging through a deeper understanding of its underlying mechanisms. The open challenge for mode averaging is the choice of modes that lead to the most optimal results, particularly if we wish to use pairs of modes to ensure that there are enough mode groups that can be used to transmit different signals in MDM.

One of the methods previously used to determine OAM mode combinations involving two to six modes calculated the correlation coefficient of the fluctuation of the intensity of an investigated mode and the crosstalk that has spread into surrounding modes [14,15]. The modes whose crosstalk had the lowest correlations were chosen as the "best" modes with which to combine the mode that was being investigated. Another method which combined three modes simply took into account the spread of crosstalk between modes [20]. Combining modes using either of these methods showed an increase in performance compared to when the system utilized only a single mode.

Nevertheless, while it is a natural assumption that neighboring mode combinations would result in maximal performance for receiver and transmitter mode averaging due to their proximity and potential for power coupling, this is not necessarily the case. We assert that the best mode combinations are not simply those that are nearest to each other, as others have investigated, but must be selected with consideration of their overall impact on received power, taking into account both crosstalk and MDL.

The study demonstrates this by determining the optimal mode combinations for receiver and transmitter mode averaging that maximize received power at different turbulence strengths, using both simulations and experiments. The optimal mode combinations are then implemented in a mode averaging system, and the received power is compared to that of a system without mode averaging as well as to a system with mode averaging using mode combinations from previous papers to demonstrate the effectiveness of mode averaging using optimal combinations.

We focus on the use of OAM mode pairs due to their relative ease of generation and detection, as well as their popularity. However, other higher-order modes could prove beneficial; thus, simulated results are also shown for LG-LG and HG-HG combinations. Additionally, previous studies have shown that there is a possible difference in the effects of turbulence on HG and LG modes [9,21,22] and have described the completeness property (described in Section 2), which provides a kind of implicit mode averaging among different mode bases. Therefore, we also briefly investigate mode averaging using LG-HG combinations.

2. BACKGROUND

For the reader's convenience, here we provide a brief summary on the modes we used (Section 2.A) as well as turbulence (Section 2.B), with detail in papers such as [3,23].

A. Higher-Order Structured Modes

Gaussian beams can be modulated to create higher-order scalar modes [24]. Two of the most well-known higher order-mode sets include the LG mode set and the HG mode set [24,25]. These mode sets represent a group of solutions to the paraxial Helmholtz wave equation solved using cylindrically symmetrical (ρ, ϕ, z) coordinates and Cartesian (x, y, z) coordinates, respectively. The LG mode set at $z = 0$ can be represented by the following equation:

$$\mathrm{LG}_p^{\ell}(\rho, \phi) = C_{\ell,p}^{\mathrm{LG}} \left(\frac{\rho\sqrt{2}}{w_0}\right)^{|\ell|} L_p^{|\ell|}\left(\frac{2\rho^2}{w_0^2}\right) \exp\left(-\frac{\rho^2}{w_0^2}\right) \exp(-i\ell\phi). \tag{1}$$

On the other hand, the HG mode set can be represented by the following equation:

$$\mathrm{HG}_{nm}(x, y) = C_{n,m}^{\mathrm{HG}} H_n\left(\frac{x\sqrt{2}}{w_0}\right) H_m\left(\frac{y\sqrt{2}}{w_0}\right) \exp\left(-\frac{x^2+y^2}{w_0^2}\right). \tag{2}$$

$L_p^{|\ell|}(\cdot)$ is the Laguerre polynomial, and $H_n(\cdot)$ and $H_m(\cdot)$ are the Hermite polynomials. w_0 is the beam waist at $z = 0$. LG beams are characterized by two parameters, namely the azimuthal index or topological charge (ℓ) and the radial index (p) [25]. ℓ defines the number of rotations of the phase about the optical axis, and p affects the number of rings (radial nodes) in the intensity profile. When $p = 0$, the set of modes is known as the OAM mode set [25]. HG beams are characterized by the n and m parameters, which define the number of rows and columns in the beam, respectively [24].

Beams that have the same beam propagation factor, M^2, diverge similarly, and so the size of the beam at the receiving aperture is the same (ignoring turbulence effects). This is important in a mode averaging system where the size of the receive aperture is likely of key importance, and so modes with similar or lower beam propagation factors would be desirable although not necessary. M^2 is given by [26]

$$M^2 = n + m + 1 = 2p + |\ell| + 1. \tag{3}$$

Any mode from one orthonormal basis can be expressed as a linear combination (weighted by phase and amplitude) of

modes (with the same beam propagation factor) from another basis [27]. This is known as the completeness property and allows an LG mode to be transformed into a set HG modes using the following equation:

$$\mathrm{LG}_{nm}(x, y, z) = \sum_{k=0}^{N} i^k b(n, m, k)\mathrm{HG}_{N-k,k}(x, y, z), \quad (4)$$

where

$$b(n, m, k) = \left[\frac{(N-k)!k!}{2^N n!m!}\right]^{\frac{1}{2}} \frac{1}{k} \times \frac{d^k}{dt^k}[(1-t)^n(1+t)^m]|_{t=0}. \quad (5)$$

In the equations, $N = M^2 - 1$, and n and m are used to characterize LG modes rather than ℓ and p. However, the indices can be recovered using $\ell = n + m$ and $p = \min(n, m)$. The power weightings and phases of HG modes making up some LG modes can be seen in Fig. 1.

B. Spatial Modes in Atmospheric Turbulence

Atmospheric turbulence is caused as a result of air of different temperatures and density mixing. This causes random space and time-varying changes in the refractive index of the air [28], which aberrates laser beams propagating through these regions.

The strength of turbulence can be conveniently characterized by the Strehl ratio (SR). It is a measure of the (on-average) ratio between the intensity of a Gaussian beam with and without the effects of turbulence. The SR is a value between zero and one with lower SR representing higher turbulence strengths. SR is defined by [3,29]

$$\mathrm{SR} = \frac{\langle I(\mathbf{0})\rangle}{I_0(\mathbf{0})}, \quad (6)$$

where $\langle I(\mathbf{0})\rangle$ is the average on-axis intensity of the beam with turbulence and $I_0(\mathbf{0})$ is the on-axis intensity without turbulence.

As mentioned in the introduction, spatial modes are susceptible to the effects of atmospheric turbulence [3]. Turbulence causes power within a transmitted mode to couple to its neighboring modes, causing crosstalk. The effect of turbulence on a mode is often characterized using a crosstalk matrix, which shows this spread of power between modes and is calculated experimentally using modal decomposition. Modal decomposition involves determining the sum of modes which constitute a given field by measuring the amplitude weightings and phases of those modes [23]. It is possible to express any field as a sum of modes which are within a complete basis. This can be described by

$$U(\boldsymbol{x}) = \sum_n c_n \Psi_n(\boldsymbol{x}), \quad (7)$$

where $U(\cdot)$ is the field that is being expressed as a sum of other modes, $\boldsymbol{x}$ is a vector describing the position of a point, subscript n describes the mode indices, c_n is the expansion coefficient for mode n of a particular basis, and $\Psi_n(\boldsymbol{x})$ is the mode n within the complete basis. The expansion coefficient is a complex number in which the amplitude describes the degree to which the field correlates to the basis mode. Modal decomposition is performed by determining the inner-product between the field and the modes making up a complete basis, and is described using the following equation:

$$c_n = \langle \Psi_n | U \rangle = \int \mathrm{d}^2\boldsymbol{x} \Psi_n^*(\boldsymbol{x}) U(\boldsymbol{x}). \quad (8)$$

In this equation, $\Psi_n^*(\boldsymbol{x})$ is the conjugate of $\Psi_n(\boldsymbol{x})$. The inner product can be used to determine between which modes crosstalk occurs by measuring the correlation between the mode that has passed through turbulence and the adjacent modes.

c_n for the transmitted mode can be used to determine the MDL of the mode. The MDL, which in a sense is a measure similar to SR but for higher-order modes, measures the apparent attenuation of a mode due to crosstalk [3,6]. It is given on-average by the following equation:

$$\mathrm{MDL}_i = 1 - \frac{\langle S_i \rangle}{S_0}. \quad (9)$$

This equation calculates the decrease in the intensity of a particular mode i, where S_i is the intensity of mode i in the presence of turbulence—this is to c_i when mode i is transmitted. S_0 is the intensity of the mode in the absence of turbulence.

3. EXPERIMENTAL METHODOLOGY

In receiver and transmitter mode averaging, two modes are transmitted and detected simultaneously. Selecting optimal modes for combinations at both the transmitter and receiver is crucial for maximizing performance. In this study, optimal modes for a select set of OAM, LG, and HG modes used within a two-mode mode averaging system are determined. The modes utilized in the study can be seen in Table 1 and have been selected

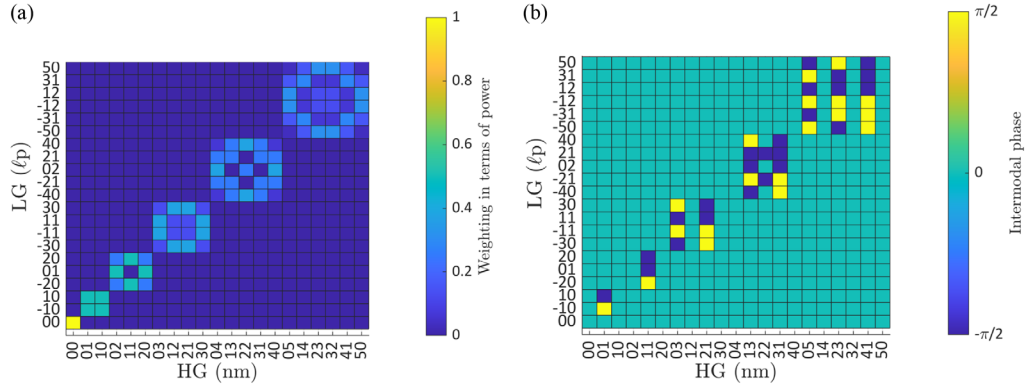


Fig. 1. (a) The power weightings and (b) the phases of HG modes making up different LG modes determined using Eqs. (4) and (5).

Table 1. LG_p^ℓ and HG_{nm} Modes That Are Investigated

M^2	LG modes	HG modes
1	LG_0^0	HG_{00}
2	LG_0^1, LG_0^{-1}	HG_{01}, HG_{10}
3	$LG_0^2, LG_0^{-2}, LG_1^0$	$HG_{02}, HG_{11}, HG_{20}$
4	$LG_0^3, LG_0^{-3}, LG_1^1, LG_1^{-1}$	$HG_{03}, HG_{12}, HG_{21}, HG_{30}$
5	$LG_0^4, LG_0^{-4}, LG_2^0, LG_1^2, LG_1^{-2}$	$HG_{04}, HG_{13}, HG_{22}, HG_{31}, HG_{40}$
6	$LG_0^5, LG_0^{-5}, LG_2^1, LG_2^{-1}, LG_1^3, LG_1^{-3}$	$HG_{05}, HG_{14}, HG_{23}, HG_{32}, HG_{41}, HG_{50}$

based on a limitation on the maximum beam propagation factor imposed by the various apertures of the experiment [30].

The "best" mode (optimal mode) to combine with a given mode (chosen mode) at different turbulence strengths is determined by measuring the received powers of all possible combinations for the given mode using the select set of modes shown in Table 1 in a mode averaging system. This means that the two modes in a mode combination are transmitted simultaneously into the turbulent channel and the power received from these modes is measured simultaneously. The mode combinations include two OAM modes, two LG modes, two HG modes, or an LG and HG mode. The maximum received power for each mode using the optimal combination is also compared to the power received when the mode is transmitted and received independently. The OAM mode combinations are explored through both experimental and simulation methods, while the LG and HG modes are investigated solely via simulation.

The measurement setup used can be seen in Fig. 2. It allows for the generation of a mode or mode combinations, the addition of turbulence, the propagation of the mode combination (when required), and the detection of modes and the powers within modes via modal decomposition.

Modes for systems using no mode averaging and mode combinations for mode averaging are first generated. Experimentally, this is performed by a beam with a wavelength of 520.2 nm by the first SLMs. In the mode averaging system beams are combined with equal weightings necessitating equal power distribution among the modes. In the simulations, powers are normalized, while experimentally, mode powers are adjusted to match the power of the Gaussian beam by modifying the grating depth on the first SLM.

Turbulence is introduced via phase screens generated using the Kolmogorov method described in [31]. Phase screens for nine turbulence strengths are generated starting with an SR of 0.1 and ending in 0.9 incrementing in steps of 0.1. It must be noted that turbulence produced using a single phase screen is not accurate for high turbulence strengths [32], but is nevertheless a common and valid experimental approach.

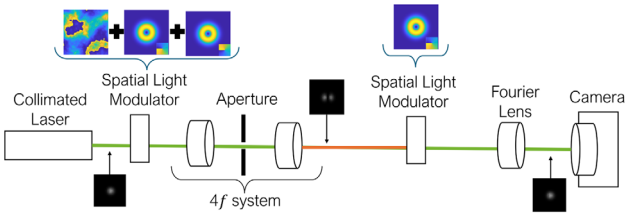


Fig. 2. The setup used to create beams, propagate the beams, and perform modal decomposition on the beams. Experimentally, propagation occurs between the $4f$ system and the second SLM as shown by the orange line. The insets show an example of the intensity of the beam along the setup, and the diagrams above SLMs show what is displayed without the grating on the SLM.

For the simulations, one hundred phase screens of each SR are generated and applied to each of the beam combinations. Thirteen million measurements must be performed if one hundred phase screens are used, and measurements are taken for all beam combinations using modal decomposition. This can be performed using simulations as the speed of the measurements is only limited by the speed of the computer performing the measurements; however, experimentally this is impractical due to the limitations on speed imposed by SLMs. Based on the simulations, modes that are indicative of the trends are chosen for a more detailed experimental study.

The detailed study involves using a hundred phase screens to determine the optimal mode combinations for two cases, namely, the $\ell = -3$ an $\ell = 1$ beams. Thirty phase screens of each turbulence strength are used for the rest of the cases in order to acquire results that would allow for a comparison between a mode averaging system and one using no mode averaging.

Finally, average crosstalk matrices for each mode combination and for single modes are determined using modal decomposition with the second SLM and a camera. For LG-HG combinations, crosstalk matrices for HG modes are specifically acquired. The resultant data allow one to ascertain the "best" mode combinations that maximize power for a given mode combination type, comparing these results to those obtained when transmitting a single mode. This setup is verified by performing modal decomposition without turbulence.

Propagation between the $4f$ system and the second SLM (indicated by an orange line in Fig. 2) varies; simulations occur in the near-field for simplicity, while experiments are conducted in the far-field, validated by the beam's propagation distance (110 cm) exceeding its Rayleigh length (10 cm). In the "thin phase screen approximation" method used in this study, the phase screen introduces turbulence, and in the experiment the propagation transitions the beam from the near-field to the far-field. This is because in the near-field, the phase screens primarily affect the phase of the beam, while in the far-field, they impact both the phase and amplitude, more closely mimicking how real turbulence influences beams [33].

4. RESULTS

In this section, we present the optimal mode combinations determined for OAM-OAM, LG-LG, HG-HG, and LG-HG mode combinations. We also compare the received powers when optimal mode combinations are used in a mode averaging system to those when only a single mode is used.

A. OAM Optimal Mode Combinations

In this section, we examine the optimal mode combinations for orbital angular momentum (OAM) modes in mode averaging systems under varying turbulence strengths. The total powers received with simulations when OAM modes are transmitted and combined with other OAM modes at different turbulence strengths can be seen in Fig. 3. Each diagram represents a specific

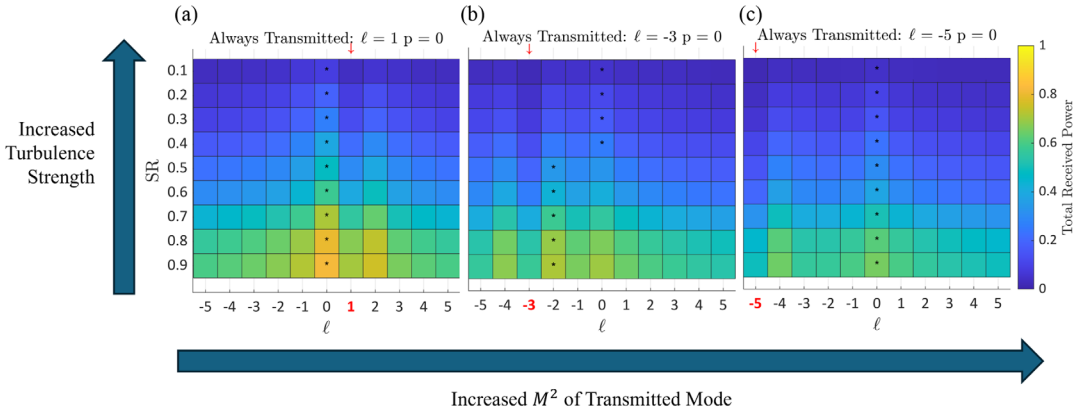


Fig. 3. Total powers received when an OAM beam is both transmitted and received with other beams at different turbulence strengths using simulations. The red arrow shows the transmitted mode, and the asterisks show with which mode a transmitted mode should be combined to maximize power. In (a) the transmitted mode is $\ell = 1$, which has the lowest M^2, in (b) $\ell = -3$, and in (c) $\ell = -5$ (highest M^2). At lower M^2 and turbulence strengths, the optimal mode combination involves the neighboring mode, whereas at higher M^2 and turbulence strengths the optimal mode is the Gaussian beam.

chosen mode, as indicated by the titles. The chosen mode is the mode for which we are trying to find the optimal mode that maximizes power. The columns correspond to the modes combined with the chosen mode, while the rows represent increasing turbulence strengths from bottom to top. Each cell displays the received power for that mode combination. The red arrow indicates the chosen mode, and the asterisk (*) marks the mode that maximizes received power when combined with the chosen mode. The three diagrams shown in the figure illustrate results for chosen modes with increasing M^2 values.

For the mode with the lowest M^2 value [Fig. 3(a)], it can be seen that the optimal combination always involves the smaller neighboring mode, regardless of turbulence strength. The *neighboring mode* refers to the mode whose ℓ value differs by one from the chosen mode. In the diagram, the Gaussian beam happens to be the neighboring mode of the chosen mode ($\ell = 1$). In Fig. 3(b), the findings for a larger chosen mode are shown. The optimal mode is the smaller neighboring mode only at lower turbulence levels. As turbulence strength increases, the optimal mode shifts from the neighboring mode to the Gaussian mode. This shift occurs at lower turbulence strengths for modes with higher M^2 values. When the M^2 value is sufficiently large [Fig. 3(c)], the Gaussian beam consistently forms part of the optimal mode combination, irrespective of turbulence strength.

To validate these simulation findings, we conducted experiments under similar conditions, as shown in Fig. 4. Similar trends as those observed in simulation findings are observed in the experimental data for $\ell = 1$ and $\ell = -3$. When the M^2 value is low [Fig. 4(a)], one of the neighboring modes is the optimal mode. However, as the M^2 value of the chosen mode and turbulence strength increases, the optimal mode shifts from a neighboring mode to a smaller mode. As can be seen in Fig. 4(b) where the chosen mode is $\ell = -3$, the optimal mode changes from the $\ell = -2$ mode to an $\ell = -1$ mode. Comparing these results to the simulation results in Figs. 3(a) and 3(b), it can be seen that there are differences between the two findings. These discrepancies are explained in Section 5.

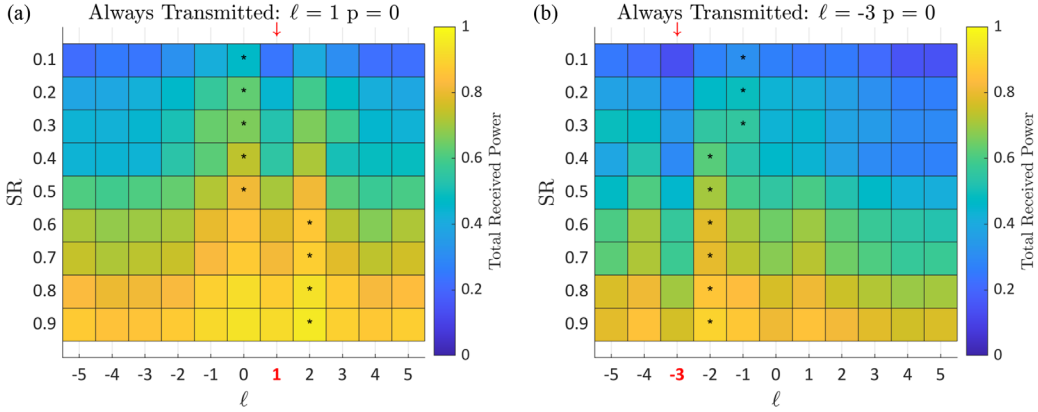


Fig. 4. Total powers received when a chosen OAM beam is both transmitted and received with other beams in an experiment. In (a) the transmitted mode is $\ell = 1$ whereas in (b) the transmitted mode is $\ell = -3$. In (a) the optimal mode is always the neighboring mode, whereas in (b) the optimal mode changes from the neighboring modes to an $\ell = -1$ mode as the turbulence strength increases. These results are slightly different to the simulation results.

B. HG and LG Optimal Mode Combinations

In this section, we examine the optimal mode combinations for various other mode combinations in mode averaging systems under varying turbulence strengths. Figure 5 illustrates the total received powers for various LG-LG, HG-HG, and LG-HG mode combinations at two different Strehl ratios: a high SR of 0.8 and a low SR of 0.4. In each plot, the chosen mode is marked by an "X," and the optimal mode with which the chosen mode should be combined to maximize power is indicated by an "*." For LG-HG modes, multiple "X"s are present because a single LG mode comprises several HG modes as per Eq. (4).

For LG-LG mode combinations where the chosen mode has $p \neq 0$, we observed that the optimal mode to combine with is consistently the Gaussian beam, regardless of the turbulence strength. For HG-HG mode combinations, the optimal mode again depends on the M^2 value of the chosen mode as well as the turbulence strength. At a low M^2 value the smaller neighboring mode forms part of the optimal mode combination. Here, the *neighboring* mode refers to the mode whose n or m value differs by one from the chosen mode. As the M^2 value increases ($\mathrm{HG}_{n=2,m=0}$ in Fig. 5) and the turbulence strength increases, the optimal mode shifts from a neighboring mode to a Gaussian mode. Beyond $M^2 = 5$, the Gaussian mode is consistently the optimal mode. This is only the case when n or m is equal to zero. When both m and n are non-zero then the optimal mode is always a Gaussian as is shown in the diagram for $\mathrm{HG}_{n=2,m=0}$ in Fig. 5).

LG-HG mode combinations follow similar trends to HG-HG modes. However, only modes with an M^2 of less than 4 have neighboring modes as optimal mode combinations at lower turbulence strengths (both examples shown for LG-HG mode combinations). It is interesting to note that the mode that is neighboring is not always the same for LG-HG modes even when the same HG modes make up the chosen LG mode.

C. Mode Averaging Power Comparison

We compare the maximum received power for each mode when using optimal mode combinations in receiver and transmitter mode averaging to that of a system without mode averaging, where only a single mode is transmitted. Figures 6(a) and 6(b)

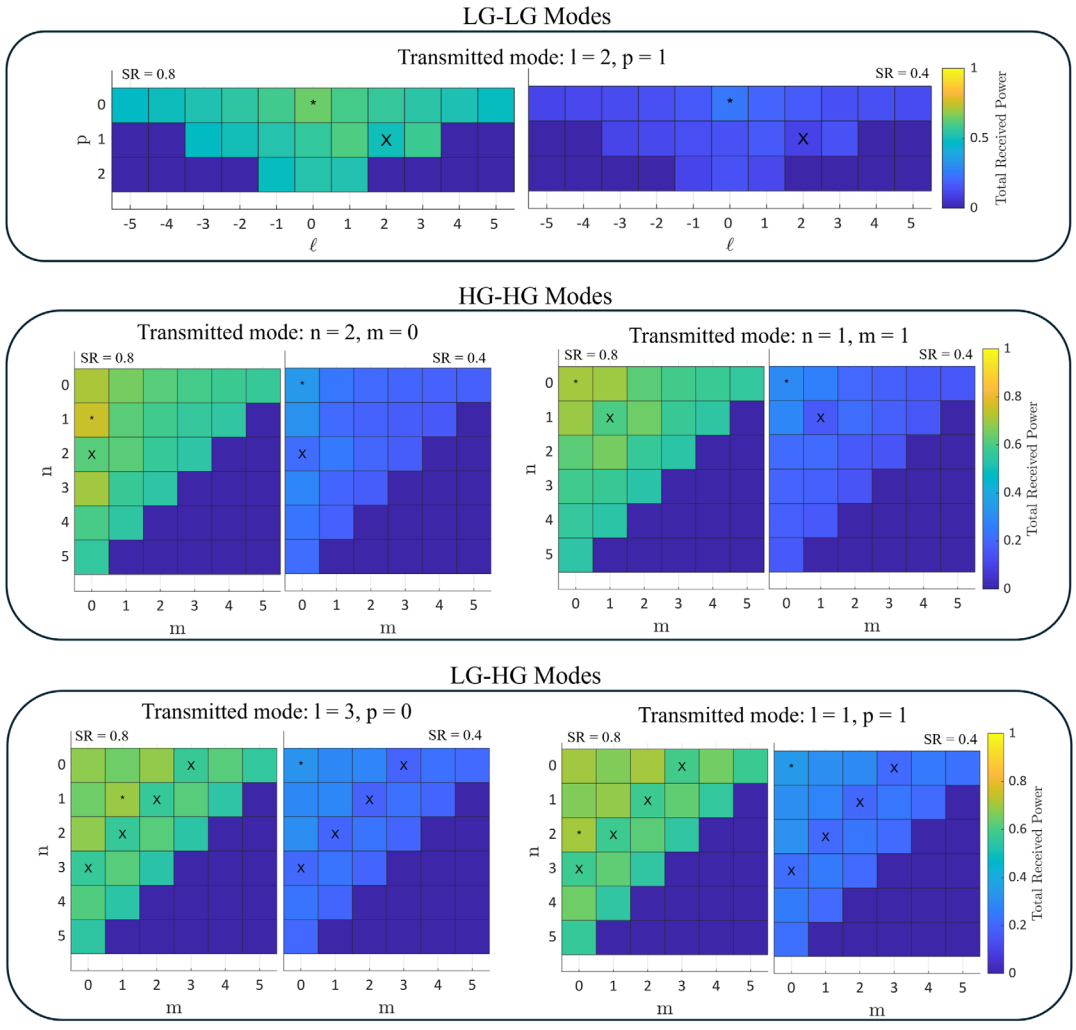


Fig. 5. Total powers received for an LG-LG mode combination, two HG-HG mode combinations, and two LG-HG mode combinations at an SR of 0.8 and 0.4. The "X" marks the chosen mode, and the "*" indicates which mode is the mode with which the transmitted mode should be combined to maximize power in a mode averaging system. It can be seen that the best mode is either a neighboring mode or a Gaussian beam, similar to the OAM modes. The definition of "neighboring mode" varies for different mode combinations.

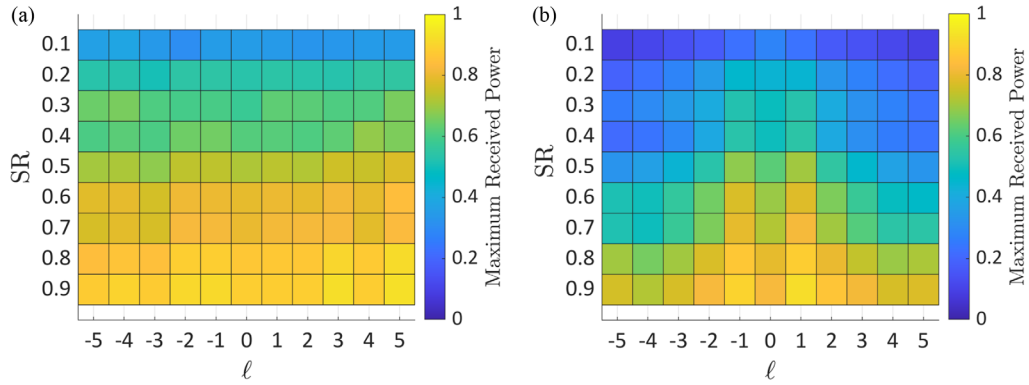


Fig. 6. The maximum average received power for different OAM modes at various turbulence strengths in a system using (*a*) optimal mode combinations in receiver and transmitter mode averaging, and (*b*) no mode averaging. Mode averaging improves the received power for most modes, particularly at higher turbulence strengths.

present the maximal power received for OAM modes obtained from the experimental setup when mode averaging is used and when no mode averaging is used, respectively. By comparing Figs. 6(a) and 6(b), it can be seen that even though the received power still decreases with turbulence strength, in both figures most modes have a greater received power when mode averaging is used than when it is not. This trend is particularly noticeable for modes with higher M^2 values and those at higher turbulence strengths. For example, for the $\ell = 3$ mode, the percentage increase for receiver and transmitter mode averaging as compared with no mode averaging is 15.7% at an SR of 0.9 and 78% at an SR of 0.1.

We also obtained simulation results for the maximum received power using LG-LG and LG-HG mode combinations at an SR of 0.6, as shown in Fig. 7. The figure also displays the maximal power for LG modes with no mode averaging and for LG-LG mode combinations which lead to the least amount of power in a mode averaging system. By comparing the received power with and without mode averaging in Fig. 7, it can be seen that mode averaging using both LG-LG and LG-HG optimal mode combinations results in higher received power. Additionally, when mode averaging is performed using mode combinations that minimize power, the received power is less than that of a system without mode averaging. The decrease in the power received when the worst mode combinations are used as compared to when the optimal mode combinations are used can range between 22.1% for a Gaussian beam and 30.7% for a $\ell = 1$, $p = 0$ mode at an SR of 0.9, and between 61.3% for a Gaussian beam and 116.42% for a $\ell = 1$, $p = 2$ mode at an SR of 0.1.

For modes where the optimal mode is not a neighboring mode, using the optimal mode instead of neighboring modes can lead to an improvement in received powers. Figure 8 shows that even though for OAM modes at lower turbulence strengths this improvement is quite small, it increases as the turbulence strength increases. For example, for an $\ell = 5$ OAM mode the difference can range from 1.26% to 21.26%. For LG modes this improvement can be quite significant. For an LG mode with $p = 2$ and $\ell = 1$, the percentage improvement can range from 12.68% at an SR of 0.9 to 71.78% at an SR of 0.1. This is also

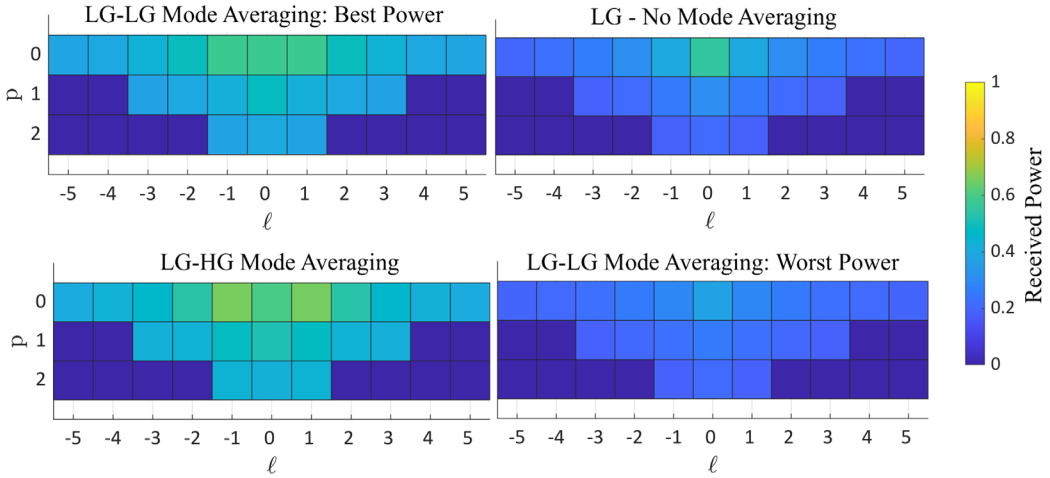


Fig. 7. Maximum received power for each transmitted LG mode at an SR of 0.6, comparing four scenarios: (a) mode averaging with the optimal LG-LG mode combination, (b) mode averaging with the optimal LG-HG mode combination, (c) no mode averaging, and (d) mode averaging with an LG-LG combination that minimizes power. It can be seen that mode averaging using the optimal LG-LG and LG-HG mode combinations perform better than no mode averaging. However, if the least optimal modes are used, the resulting power from mode averaging may be worse than without mode averaging.

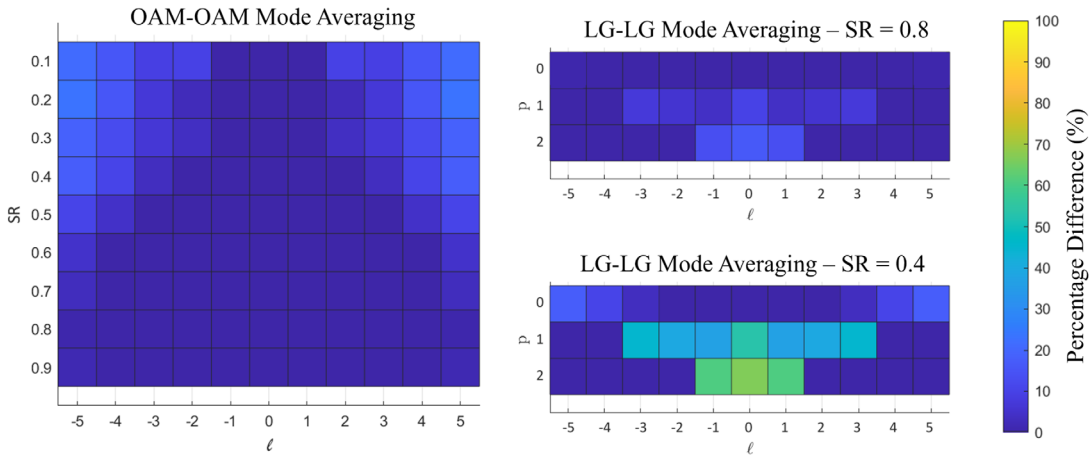


Fig. 8. The percentage difference between the power acquired when the optimal mode is used and the power acquired when the neighboring mode is used for OAM-OAM and LG-LG mode combinations in the simulations. At low turbulence strengths the difference is low; however, as the turbulence strength increases the percentage becomes significant. This is, particularly, the case for LG modes with larger p values. It must be noted that when the percentage is 0% the optimal mode is the neighboring mode.

the case for HG-HG and LG-HG mode combinations though in some cases it is difficult to define what a neighboring mode is.

5. DISCUSSION

In this section, we discuss the implications of our findings for OAM-OAM, LG-LG, HG-HG, and LG-HG mode combinations, and how they relate to previous studies.

A. OAM Mode Combinations

In the Section 4, we showed that for all mode combinations at lower M^2 values and lower turbulence levels, the optimal mode is a neighboring mode. However, as the M^2 value and/or turbulence level increases, the optimal mode often changes. This indicates that optimal mode combinations depend on both the M^2 value of the chosen mode and the turbulence strength. Consequently, the optimal mode combination is not always the neighboring mode, contrary to suggestions in previous studies [14,15,20].

It is not surprising that at lower M^2 values and lower turbulence strengths the optimal mode combination is the neighboring mode. Typically, crosstalk from the chosen mode predominantly spreads into neighboring modes, so combining with neighboring modes should theoretically result in higher received power [34].

However, it is unexpected that only the lower neighboring mode is the optimal mode in our simulations, as crosstalk should spread symmetrically into both neighboring modes [28]. Additionally, the shift in the optimal mode as M^2 or turbulence increases deviates from expectations if crosstalk were the only factor influencing the received power, suggesting that other factors are at play.

These observations can be explained by considering the mode-dependent loss (MDL) of the modes [the amount of power lost from the modes calculated using Eq. (9)]. In this study, performance is measured using the received power, which is directly affected by MDL. In receiver and transmitter mode averaging, the laser power is divided equally between the two modes at the transmitter. The MDL of these two modes contributes equally to the average MDL of the system. As a result, it becomes favorable to choose modes with lower M^2 values and, consequently, lower MDL to minimize the average MDL. The crosstalk that spreads between the two modes in a mode combination can also decrease the average MDL. Therefore, the objective when selecting optimal modes is to find the combination that lowers the average MDL the most.

Figure 9 illustrates how MDL changes with M^2 and turbulence strength. As M^2 increases, the beam size also increases, making the beams more susceptible to turbulence-induced distortions. Increased turbulence leads to more crosstalk and higher MDL.

For chosen modes where the neighboring mode is the optimal mode, the chosen mode has a smaller M^2 value. Since modes that have a smaller M^2 value also have a lower MDL [as can be seen in Fig. 9(a)], the average MDL will be low. The crosstalk that spreads between modes helps to further decrease the average MDL. Since most of the crosstalk spreads into neighboring modes, the optimal mode is one of the neighboring modes. The neighboring mode with a lower M^2 contributes to a lower average MDL. Thus, the optimal mode combination will include the smaller mode.

In contrast, for modes where the neighboring mode is no longer optimal, the chosen mode has a higher M^2 value or is subjected to higher turbulence strength. This means that the MDL of both the chosen mode and its neighboring modes is also high. While the crosstalk increases for these modes [34], the efficiency with which crosstalk can mitigate the MDL decreases as M^2 or turbulence strength increases because the crosstalk also spreads to more modes. At this point, it becomes more favorable to combine the chosen mode with the mode that has the lowest MDL—even if very little crosstalk occurs between them. This is the case for the mode combination including an $\ell = 5$ mode and an $\ell = 0$ mode.

The turbulence threshold at which crosstalk ceases to be the dominant factor in determining the optimal mode combination

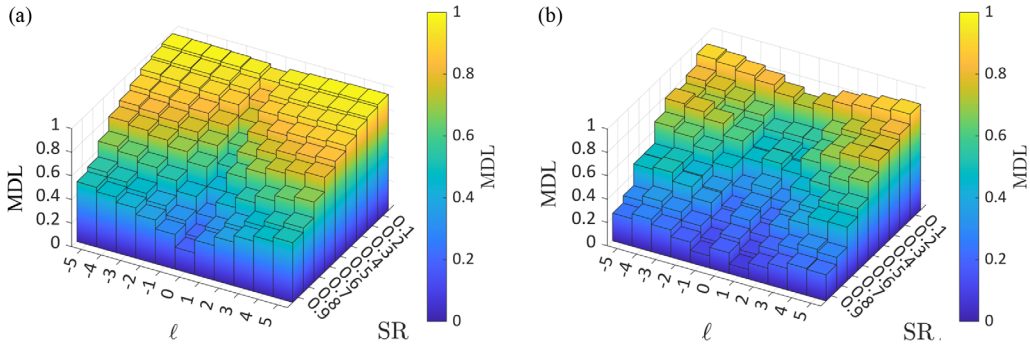


Fig. 9. The MDL of the beams measured using (*a*) simulations and (*b*) experiments. MDL must be considered when choosing optimal modes, as it increases with M^2 and turbulence strength, contributing to the average powers. The differences between the two figures explain the discrepancies between the experimental and simulation results for best mode combinations.

depends on the specific modes involved. Future research could explore the thresholds at which MDL overtakes crosstalk in greater detail, potentially leading to the development of the adaptive mode selection algorithm that adjusts to changing turbulence conditions. To achieve this, it would be valuable to model the relationship between MDL and turbulence strength.

The Gaussian mode typically has the lowest MDL. However, in Fig. 4, we observe that in the experiment, modes with higher M^2 values (e.g., $\ell = 3$) at higher turbulence strengths are combined with the $\ell = -1$ mode rather than the Gaussian beam. The deviation between experimental and simulation results, particularly the shifts in optimal modes, may be attributed to differences in MDL. Comparing Figs. 9(a) and 9(b), we see that in the experimental results, the MDL of the $\ell = -1$ mode is often lower than that of the Gaussian beam. Similarly, at lower turbulence levels, the $\ell = 2$ mode appears to have a lower MDL than the Gaussian beam. This leads to the change in the neighboring mode for the $\ell = -1$ as turbulence strength increases. This indicates that, in the experiment, a lower M^2 value does not always correspond to a lower MDL, which is likely due to experimental errors and differences in propagation distance between the simulations and experiments. Nevertheless, the experimental results still follow the trends described for the simulation results.

Our findings underscore the complex interplay between MDL and crosstalk, which varies with mode characteristics and environmental conditions, challenging the assumption that neighboring modes are always optimal for mode averaging. In previous studies, neighboring modes were chosen for mode combinations based solely on crosstalk considerations [14,15,20]. Although not shown in this paper, our results indicate that the mode combination yielding the second-highest received power for chosen modes with increasing M^2 values and higher turbulence strengths is a neighboring mode in most cases—the same combination utilized in past studies. While, in past research, the mode combinations including neighboring modes showed improved performance, it is likely that they did not achieve the maximum possible performance especially for higher turbulence levels and for modes at higher M^2 values.

The improvement could be significant, as our results suggest that the optimal mode combinations, which are not always neighboring modes, can yield higher received power compared to neighboring mode combinations. This means using optimal mode combinations could be especially useful for long propagation distance where turbulence levels are high [29].

Previous studies used metrics such as bit error rate (BER) and outage probability, which means the papers are not directly comparable to this work. It would be beneficial to use optimal mode combinations in a communication system and measure BER and outage probability to allow for a direct comparison.

However, if mode averaging is implemented in a communication system utilizing mode-division multiplexing (MDM), using the optimal mode for each mode with a higher M^2 value may not be feasible, as it could cause interference. Therefore, it may be more practical to use a less optimal mode combination—including neighboring modes, as done in the past [20].

We are also uncertain whether the neighboring mode will still produce the second-best received power at very high M^2 values. It is likely that this will not be the case, as crosstalk spreads more at higher M^2 values, meaning that most of the crosstalk may not spread into a neighboring mode. The current study is limited by the range of ℓ values used. Investigating this further could provide valuable insights into mode selection at higher M^2 values.

B. Other Mode Combinations

Our findings demonstrate that the optimal mode combinations for maximizing received power using LG-LG, HG-HG, and LG-HG modes follow the same general trends observed for OAM modes. This similarity is attributed to MDL, which influences the results across all these mode combinations. MDL exhibits consistent trends with increasing M^2 values and turbulence strengths for both LG and HG modes. Notably, for LG modes, the radial index p contributes twice as much to the M^2 value as the azimuthal index, ℓ, as shown in Eq. (3). Consequently, LG modes with higher p values behave similarly to OAM modes with large ℓ values.

The main difference between these mode combinations lies in the definition of the neighboring mode at lower M^2 values and turbulence strength. As was specified in Section 4, for OAM and LG mode combinations, the neighboring mode typically refers to the mode with an adjacent ℓ value. In contrast, for HG and HG-LG mode combinations, the neighboring mode refers to the mode with an adjacent n or m value, depending on

whether m or n is equal to zero. The optimal neighboring mode for LG-LG and HG-HG mode combinations is normally the one with the least MDL.

Determining the optimal neighboring mode for LG-HG mode combinations is more complex due to the nature of the mode combination. The complexity arises because a single LG mode can be represented as a superposition of several HG modes with the same M^2, but with different weightings. This means that a transmitted HG mode is effectively combined with the multiple HG modes that formed the LG mode, as illustrated in the crosstalk matrices for the LG-HG mode combinations in Fig. 5. The differing weightings result in some HG modes having more power than others, leading to varying amounts of crosstalk. Therefore, the neighboring mode that provides the largest received power is the smaller one, which most closely aligns with the HG modes that have the highest initial power due to the LG mode transformation. In Fig. 5, two different LG modes composed of the same HG modes are shown, but the neighboring modes that provide maximal power when combined with the LG mode differ. If all HG modes had the same weighting, any of the neighboring modes could potentially be the optimal choice.

Since OAM modes are a subset of LG modes, and LG modes can be transformed into a set of HG modes, it is not surprising that the optimal combinations for LG-LG, HG-HG, and LG-HG mode pairs are similar to those found for OAM mode combinations. This interrelation underscores the fundamental nature of MDL and crosstalk effects in mode-averaging systems.

It is also not surprising that mode averaging using optimal modes with LG-LG, HG-HG, and LG-HG can lead to a significant improvement in received power especially for higher turbulence strengths and large M^2 values as was shown to be the case for OAM-OAM mode combinations. The results shown here cannot be verified with a comparison to past papers as there is no research into using HG or large LG modes for mode averaging.

Nevertheless, it is, perhaps, interesting that the maximum power for mode averaging using LG-HG modes is higher than that obtained for LG-LG modes for several cases. This is particularly significant for modes that are best combined with neighboring modes, as it suggests that simply changing the mode basis used to measure the incoming beam could increase the amount of crosstalk collected from the Gaussian beam. This advantage may imply that the HG and LG modes are affected differently by turbulence as was shown in this paper [21]. These findings indicate potential benefits in exploring different mode combinations for improving system performance using mode averaging. Further experimental investigation into these mode combinations would be favorable.

The study using simulations was limited by the simplified turbulence model, which is not accurate for higher turbulence strengths. Incorporating more complex propagation techniques, such as the split-step Fourier method [32], or validating the results using experimentation with real-world turbulence patterns could provide further insights. Future research could explore these avenues to enhance the understanding of optimal mode combinations under various atmospheric conditions.

6. CONCLUSION

In the past, mode combinations for receiver and transmitter mode averaging were determined based on crosstalk. In this study, we demonstrate the importance of also considering MDL when selecting modes. This is achieved by measuring the received power for systems using mode combinations involving two OAM modes, two LG modes, two HG modes, or a combination of LG and HG modes, and determining which combinations maximize power. Through this approach, we gain a deeper understanding of the underlying mechanisms of mode averaging.

Our investigation further demonstrates that employing optimal mode combinations in a mode averaging system can significantly enhance received power across all mode combinations studied. The enhancement in received power is more pronounced at higher turbulence strengths and for modes with higher M^2 values. This suggests that mode averaging using optimal modes is particularly effective under conditions where turbulence impacts transmission more severely, such as long propagation distances. In practical communication systems, these improvements in average received power are significant, as they ensure the power collected by the receiver remains above operational thresholds over time, enhancing both reliability and efficiency.

Our results also indicate that if random modes are chosen, they may lead to a decrease in received power compared to a system without mode averaging. Therefore, selecting optimal mode combinations is essential for maximizing received power in optical communication systems, necessitating a careful balance between crosstalk and MDL. Additionally, our findings suggest that exploring different mode bases and combinations, such as LG-HG modes, may offer further benefits and warrants future investigation.

Funding. National Research Foundation (MND200513521703, TTK2204011621).

Disclosures. The authors declare no conflicts of interest.

Data availability. Data underlying the results presented in this paper are not publicly available at this time but may be obtained from the authors upon reasonable request.

REFERENCES

1. Z. Hu, Y. Li, Z. Chen, *et al.*, "Aiming for high-capacity multi-modal free-space optical transmission leveraging complete modal basis sets," Opt. Commun. **541**, 129531 (2023).
2. G. Gibson, J. Courtial, M. J. Padgett, *et al.*, "Free-space information transfer using light beams carrying orbital angular momentum," Opt. Express **12**, 5448–5456 (2004).
3. M. A. Cox, N. Mphuthi, I. Nape, *et al.*, "Structured light in turbulence," IEEE J. Sel. Top. Quantum Electron. **27**, 7500521 (2020).
4. A. Trichili, M. A. Cox, B. S. Ooi, *et al.*, "Roadmap to free space optics," J. Opt. Soc. Am. B **37**, A184–A201 (2020).
5. T. Weyrauch and M. A. Vorontsov, *Free-Space Laser Communications with Adaptive Optics: Atmospheric Compensation Experiments* (Springer, 2008), vol. **2**, pp. 247–271.
6. S. Li, S. Chen, C. Gao, *et al.*, "Atmospheric turbulence compensation in orbital angular momentum communications: advances and perspectives," Opt. Commun. **408**, 68–81 (2018).
7. G. L. Bastin, L. C. Andrews, R. L. Phillips, *et al.*, "Measurements of aperture averaging on bit-error-rate," Proc. SPIE **5891**, 589102 (2005).

8. S. Navidpour, M. Uysal, and M. Kavehrad, "BER performance of free-space optical transmission with spatial diversity," IEEE Trans. Wireless Commun. **6**, 2813–2819 (2007).
9. M. A. Cox, L. Cheng, C. Rosales-Guzmán, *et al.*, "Modal diversity for robust free-space optical communications," Phys. Rev. Appl. **10**, 024020 (2018).
10. A. Wang, L. Zhu, M. Deng, *et al.*, "Experimental demonstration of OAM-based transmitter mode diversity data transmission under atmosphere turbulence," Opt. Express **29**, 13171–13182 (2021).
11. H. Song, L. Li, K. Pang, *et al.*, "Demonstration of using two aperture pairs combined with multiple-mode receivers and MIMO signal processing for enhanced tolerance to turbulence and misalignment in a 10 Gbit/s QPSK FSO link," Opt. Lett. **45**, 3042–3045 (2020).
12. D. J. Geisler, T. M. Yarnall, M. L. Stevens, *et al.*, "Multi-aperture digital coherent combining for free-space optical communication receivers," Opt. Express **24**, 12661–12671 (2016).
13. D. J. Geisler, T. M. Yarnall, C. M. Schieler, *et al.*, "Ground receiver architectures enabled by digital coherent combining," in *Optics InfoBase Conference Papers Part F106* (2018), pp. 7–8.
14. S. Huang, G. R. Mehrpoor, and M. Safari, "Spatial-mode diversity and multiplexing for FSO communication with direct detection," IEEE Trans. Commun. **66**, 2079–2092 (2018).
15. E. M. Amhoud, B. S. Ooi, and M. S. Alouini, "A unified statistical model for atmospheric turbulence-induced fading in orbital angular momentum multiplexed FSO systems," IEEE Trans.Wireless Commun. **19**, 888–900 (2020).
16. L. Li, H. Song, R. Zhang, *et al.*, "Increasing system tolerance to turbulence in a 100-Gbit/s QPSK free-space optical link using both mode and space diversity," Opt. Commun. **480**, 126488 (2021).
17. L. Li, H. Song, R. Zhang, *et al.*, "Demonstration of both mode and space diversity in a 100-Gbit/s QPSK free-space optical link to increase system tolerance to turbulence," in *Optics InfoBase Conference Papers* (2019), Vol. **Part F160**, pp. 4–6.
18. M. Safari and S. Huang, "MIMO optical wireless communication via monolithic or sparse apertures," J. Opt. **20**, 024017 (2018).
19. B. B. Yousif and E. E. Elsayed, "Performance enhancement of an orbital-angular-momentum-multiplexed free-space optical link under atmospheric turbulence effects using spatial-mode multiplexing and hybrid diversity based on adaptive MIMO equalization," IEEE Access **7**, 84401–84412 (2019).
20. L. Zhu, M. Deng, B. Lu, *et al.*, "Turbulence-resistant high-capacity free-space optical communications using OAM mode group multiplexing," Opt. Express **31**, 14454–14463 (2023).
21. M. A. Cox, L. Maqondo, R. Kara, *et al.*, "The resilience of Hermite— and Laguerre–Gaussian modes in turbulence," J. Lightwave Technol. **37**, 3911–3917 (2019).
22. X. Gu, L. Chen, and M. Krenn, "Phenomenology of complex structured light in turbulent air," Opt. Express **28**, 11033–11050 (2020).
23. J. Pinnell, I. Nape, B. Sephton, *et al.*, "Modal analysis of structured light with spatial light modulators: a practical tutorial," J. Opt. Soc. Am. A **37**, C146–C160 (2020).
24. A. Siegman, *Lasers* (University Science Books, 1986).
25. L. Allen, M. W. Beijersbergen, R. J. C. Spreeuw, *et al.*, "Orbital angular momentum of light and the transformation of Laguerre-Gaussian laser modes," Phys. Rev. A **45**, 8185–8189 (1992).
26. S. Saghafi and C. Sheppard, "The beam propagation factor for higher order Gaussian beams," Opt. Commun. **153**, 207–210 (1998).
27. A. T. Oneil and J. Courtial, "Mode transformations in terms of the constituent Hermite–Gaussian or Laguerre–Gaussian modes and the variable-phase mode converter," Opt. Commun. **181**, 35–45 (2000).
28. J. A. Anguita, M. A. Neifeld, and B. V. Vasic, "Turbulence-induced channel crosstalk in an orbital angular momentum-multiplexed free-space optical link," Appl. Opt. **47**, 2414 (2008).
29. L. C. Andrews and R. L. Phillips, *Laser Beam Propagation Through Random Media*, 2nd ed. (SPIE, 2012), vol. **91**.
30. S. Restuccia, D. Giovannini, G. Gibson, *et al.*, "Comparing the information capacity of Laguerre–Gaussian and Hermite–Gaussian modal sets in a finite-aperture system," Opt. Express **24**, 27127–27136 (2016).
31. R. G. Lane, A. Glindemann, and J. C. Dainty, "Simulation of a Kolmogorov phase screen," Wave Random Media **2**, 209–224 (1992).
32. A. Belmonte, "Feasibility study for the simulation of beam propagation: consideration of coherent lidar performance," Appl. Opt. **39**, 5426–5445 (2000).
33. C. Rosales-Guzman and A. Forbes, *How to Shape Light with Spatial Light Modulators* (SPIE, 2017).
34. G. R. Mehrpoor, M. Safari, and B. Schmauss, "Free space optical communication with spatial diversity based on orbital angular momentum of light," in *4th International Workshop on Optical Wireless Communications (IWOW)* (2015), pp. 78–82.